Graphene Chemistry

International Edition: DOI: 10.1002/anie.201704419
German Edition: DOI: 10.1002/ange.201704419

Thermal Disproportionation of Oxo-Functionalized Graphene

*Fabian Grote, Christoph Gruber, Felix Börrnert, Ute Kaiser, and Siegfried Eigler**

Abstract: *Graphene production by wet chemistry is an ongoing scientific challenge. Controlled oxidation of graphite introduces oxo functional groups; this material can be processed and converted back to graphene by reductive defunctionalization. Although thermal processing yields conductive carbon, a ruptured and undefined carbon lattice is produced as a consequence of CO_2 formation. This thermal process is not understood, but it is believed that graphene is not accessible. Here, we thermally process oxo-functionalized graphene (oxo-G) with a low (4–6 %) and high degree of functionalization (50–60 %) and find on the basis of Raman spectroscopy and transmission electron microscopy performed at atomic resolution (HRTEM) that thermal processing leads predominantly to an intact carbon framework with a density of lattice defects as low as 0.8 %. We attribute this finding to reorganization effects of oxo groups. This finding holds out the prospect of thermal graphene formation from oxo-G derivatives.*

A decade after the outstanding experiments with graphene, research activities in many fields of science have emerged.[1] Graphene has applications in electronic devices,[2] supercapacitors,[3] solar cells,[4] sensors,[5] energy-storage materials,[6] bio-applications,[7] functional composites,[8] and membranes for sieving.[9] Chemical methods for the production of graphene are based on either reductive or oxidative treatment of graphite,[10] whereby oxidation is favored for the large-scale production of flakes of single layers.[11] The most prominent compound class is graphene oxide (GO). GO bears mainly hydroxyl and epoxy groups, which are located on both sides of the carbon framework, but also many defect sites.[11b] Lattice defects introduced by over-oxidation are permanent and can't be healed by thermal processing without a carbon source.[12] Various reductive defunctionalization routes have been developed and many of them efficiently produce graphene; however, the reduction agent is often difficult to remove.[13] In the view of surface purity, we recently reported on a clean method to reduce oxo-G photochemically.[14] Although thermal processing of GO is convenient, unfortunately many additional lattice defects are introduced.[13a,15] Consequently, HRTEM imaging of GO treated at 160 °C revealed an amorphous carbon lattice.[16] Those results are also supported by thermogravimetric analysis, proving CO and CO_2 formation. Raman spectroscopy performed on thermally processed GO gives also evidence for the introduction of excess defects.[13a,15] In contrast to GO, oxo-G, which we introduced more recently, bears an almost intact hexagonal carbon lattice with oxo groups as addends. Thus, oxo-G is suitable for Raman and HRTEM investigations. Here we show for the first time that graphene of reasonable quality is indeed accessible by processing oxo-G between 75–175 °C. We quantify the quality of graphene after thermal processing and find few-atoms vacancy defects next to an intact hexagonal carbon lattice and holes that formed as a consequence of the rearrangement of oxo groups on the hexagonal lattice structure.

Oxo-G, on which we reported earlier, bears a degree of functionalization (θ_F) of about 50 %.[10a] The density of lattice defects (θ_D) was determined after chemical reduction down to about 0.03 % by analyzing the I_D/I_G ratio of the defect-induced D peak and the G peak in the Raman spectra. An I_D/I_G ratio of about 1 is reached for θ_D or θ_F values of roughly 3 %. Therefore, it is impossible to analyze θ_D or θ_F of higher values using the I_D/I_G ratio. However, recently, we studied the region of θ_D or $\theta_F > 3$ % by analyzing the intensity of Raman peaks and found that the peak intensity is modulated by photoluminescence.[17] The intensity depends on θ. In first approximation θ values and Raman intensity values follow a double logarithmic behavior, which is almost linear over a wide range of θ values between 0.5 % and about 20 %.[17]

In the following, we use the change of Raman intensities upon thermal processing of oxo-G and propose a thermal decomposition pathway that leaves an intact carbon framework behind (Figure 1), along with the generation of point defects. In addition, Raman spectroscopy and HRTEM give novel insights into the lattice structure of thermally processed oxo-G for the first time.

Graphene was prepared from graphite sulfate, a stage-1 graphite intercalation compound (GIC) with an idealized formula of $(C_{24}HSO_4{\cdot}2H_2SO_4)_n$.[18] Addition of water to graphite sulfate led to hydroxyl-functionalized graphite with $\theta_F \approx 4$–6 % and the idealized formula of $(C_{24}OH{\cdot}2H_2O)_n$. Single layers could be delaminated, deposited on 300 nm SiO_2/Si wafers, and chemically reduced. Statistical Raman spectroscopy (SRS) revealed $\theta_D \approx 0.03$ % on average.[18a]

[*] Prof. Dr. S. Eigler
Institute of Chemistry and Biochemistry
Freie Universität Berlin
Takustrasse 3, 14195 Berlin (Germany)
E-mail: siegfried.eigler@fu-berlin.de
F. Grote, C. Gruber, Prof. Dr. S. Eigler
Department of Chemistry and Pharmacy
and Central Institute of Materials and Processes (ZMP)
Friedrich-Alexander-Universität Erlangen-Nürnberg, FAU
Dr.-Mack Strasse 81, 90762 Fürth (Germany)
Dr. F. Börrnert, Prof. Dr. U. Kaiser
Materialwissenschaftliche Elektronenmikroskopie
Universität Ulm
Albert-Einstein-Allee 11, 89081 Ulm (Germany)
Dr. F. Börrnert
IFW Dresden
PF 270116, 01171 Dresden (Germany)

Supporting information for this article can be found under: https://doi.org/10.1002/anie.201704419.

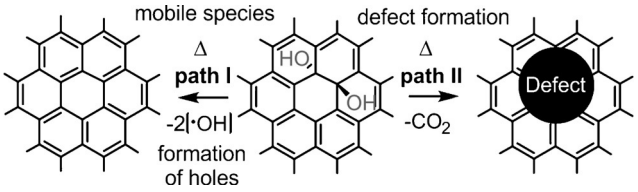

Figure 1. Reaction paths of thermally processed oxo-functionalized graphene (oxo-G). Path I: Thermal disproportionation of oxo-G into graphene and mobile oxo species, which may etch existing defects to holes a few nanometers in diameter. Path II: Direct formation of new in-plane lattice defects, accompanied by CO_2 formation.

Here, we followed this synthetic route and coated Quantifoil TEM grids with oxo-$G_{4\%}$ ($\theta_F \approx 4$–6% for functionalized monolayers) by the Langmuir–Blodgett (LB) technique.

The carbon lattice can be visualized subsequently at atomic resolution before and after thermal processing (Figure 2 and Figures S1 and S2). As shown in Figure 2 A clean and intact graphene areas approximately 5–10 nm in diameter are identified for oxo-$G_{4\%}$, which was exclusively processed at room temperature and below. In addition, some contaminations and lattice point defects are visible. The inset diffractogram shows sharp signals from the intact hexagonal lattice. Functional groups such as hydroxyl groups are very likely cleaved by the electron beam, a process that we reported earlier.[19] Next, an oxo-$G_{4\%}$-coated TEM grid was thermally treated at 270 °C in an active coal bath, a method that we introduced to remove contaminations on graphene.[20] The processing temperature should lead to defect formation and an amorphous carbon framework, as identified previously for oxo-$G_{50\%}$ (θ_F of about 50 %) and GO.[13a,15] The HRTEM image in Figure 2 B, however, reveals a surprisingly intact hexagonal carbon lattice. Also, the signals from the lattice in the diffractogram are very distinct and only slightly blurred due to some isotropic strain around the defects. In addition, point defects of mainly few-atom vacancies are identified. Also some larger holes are apparent which are barely present in the starting material. If one considers that at least one hydroxyl group of oxo-$G_{4\%}$ is present for about 24 C atoms, the formation of graphene by thermal processing needs to be revised.

As evident from Figure 2 B, thermally processed oxo-$G_{4\%}$ bears areas of intact graphene with diameters of up to 3–5 nm. Thus, we conducted statistical Raman spectroscopy (SRS) on thermally treated oxo-$G_{4\%}$. The results reveal (Figure S5) $\Gamma_{2D} = 54 \pm 14\ cm^{-1}$ and $I_D/I_G = 2.0 \pm 0.2$. These values can be assigned to an average distance between defects of about 3–4 nm, following the relation described by Lucchese and Cançado.[21] Temperature-dependent Raman spectroscopy conducted between 25 °C and 500 °C (Figure 3 A) further reveals that the formation of graphene starts at 75 °C and continues until 120 °C, as indicated by the temperature profile of the narrowing of the Γ_{2D} value and the course of the I_D/I_G ratio profile. The quality of graphene significantly decreases at temperatures above 250–300 °C, which may be a consequence of impurities reacting with the graphene lattice. Raman spectra of individual single layers of oxo-$G_{4\%}$ before and after thermal processing are depicted in Figure 3 B and

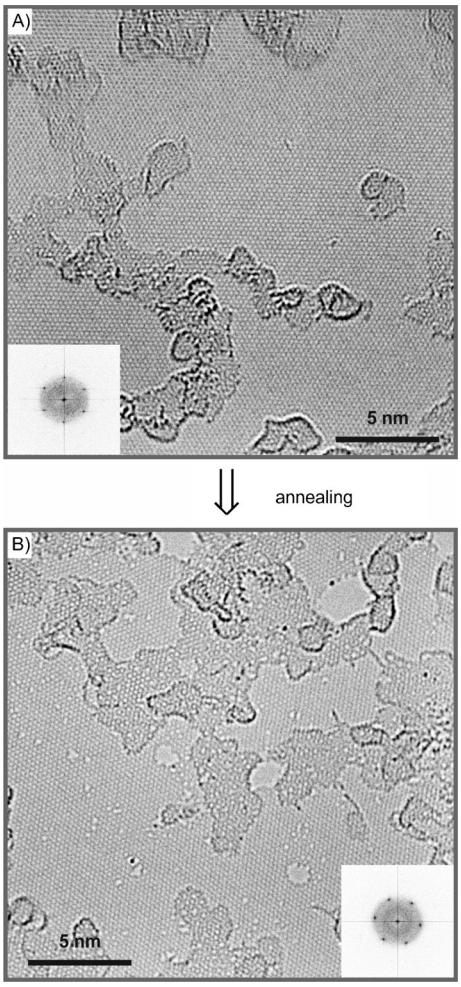

Figure 2. HRTEM images of oxo-functionalized graphene with a degree of functionalization of 4–6 % (oxo-$G_{4\%}$); insets: (Fourier transform of the respective micrograph representing its diffractogram indicating the hexagonal long-range order of the C framework). A) Hexagonal carbon framework with adsorbed contaminations and few lattice point defects. B) Lattice point defects of few atoms and holes a few nanometers in diameter are observed after annealing (see also Figures S1–S3).

Figure S5. The formation of graphene is clearly indicated by the 2D peak narrowing to $\Gamma_{2D} = 50\ cm^{-1}$.

The initial lattice defect concentration in oxo-$G_{4\%}$ can be determined after chemical reduction and SRS to $\theta_D \approx 0.03\%$ (1 defect for about 3000 C atoms, Figure S5). Consequently, the defects of thermally processed oxo-$G_{4\%}$, probed by SRS and HRTEM, are indeed thermally introduced. Assuming a minimal functionalization degree of 4 % in oxo-$G_{4\%}$, thermal processing leads to one defect upon removal of about five hydroxyl groups. Taking into account that CO_2 is formed, the results suggest that two hydroxyl groups form one defect and the other three hydroxyl groups are mobile on the surface and may either detach or more likely increase the size of point defects by CO or CO_2 formation. Consequently, intact hexagonal areas of graphene are formed next to point defects and some holes a few nanometers in diameter, as visualized in Figure 2 B.

The described processes are even more general and we find that oxo-$G_{50\%}$ behaves similarly, although the θ_D value is

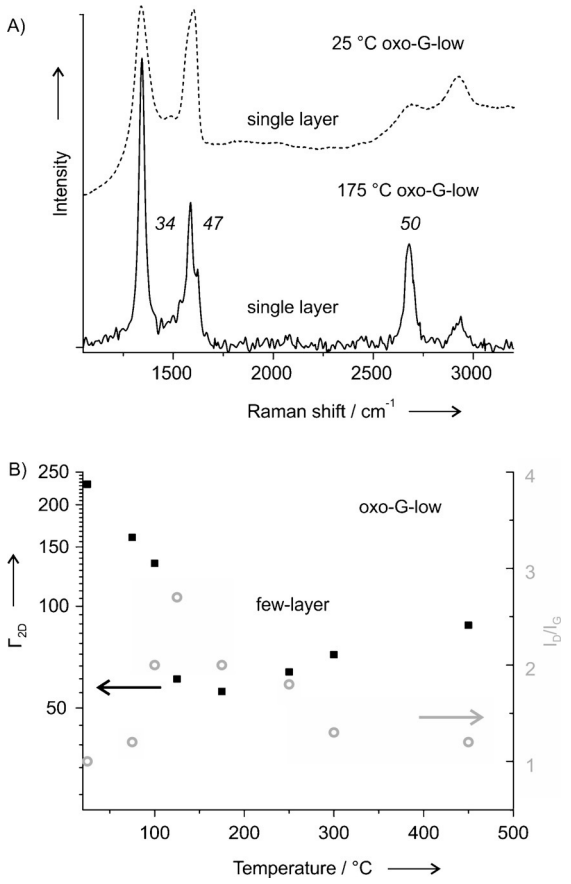

Figure 3. A) Raman spectra of single layers of oxo-$G_{4\%}$ (dashed line) at 25 °C and after thermal processing at 175 °C (solid line, italic numbers for 175 °C oxo-$G_{4\%}$: full-width at half-maximum, Γ). B) Plot of the temperature-dependent Raman spectroscopy of oxo-$G_{4\%}$ between 25 and 500 °C, showing the evolution of the I_D/I_G ratio and Γ_{2D} values (data from few-layers).

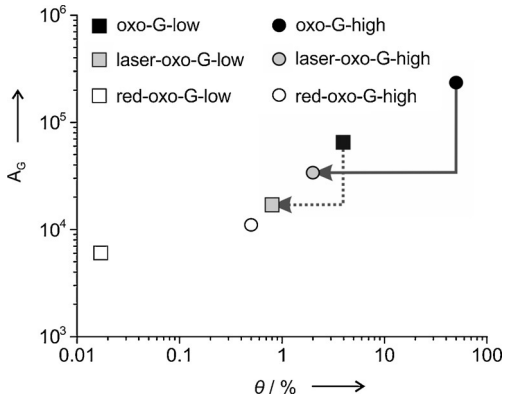

Figure 4. Plot of the integrated area (A_G) of the G peak of Raman spectra vs. the degree of functionalization (θ) upon thermal (induced by the Raman laser, 532 nm) processing and chemical reduction of oxo-$G_{4\%}$ (red-oxo-G-low) and oxo-$G_{50\%}$ (red-oxo-G-high), respectively.

higher.[10a] At high θ_F values of around 50 % we use the integrated area of the G peak (A_G) as a measure of θ, according to our recently reported analytical method.[17] The reference points of Figure 4 are taken from oxo-$G_{4\%}$ processing. The SRS analysis of chemically reduced oxo-$G_{50\%}$ (red-oxo-$G_{50\%}$) suggests $\theta_D = 0.5\,\%$ (Figure 4 and Figure S4). After thermal processing of oxo-$G_{50\%}$ the θ_D value can be estimated by the analysis of A_G (Figure 4) to be about 2 %. Considering that 0.5 % of lattice defects are already present in oxo-$G_{50\%}$, only about 1.5 % of additional lattice defects were introduced by thermal processing. Within experimental errors it can be concluded that one defect is formed upon transformation of about 30 sp^3 centers (hydroxyl and epoxy groups). This investigation suggests that the majority of functional groups of oxo-$G_{50\%}$ undergo defunctionalization resulting in a graphene lattice (Figure 1, path I) and holes. The holes may be generated by mobile epoxy and hydroxyl groups in the temperature range of 75 and 120 °C.

We demonstrated that graphene with a density of lattice defects of about 0.8 % is produced by thermal processing of oxo-functionalized graphene with a low degree of functionalization of about 4–6 %. Intact graphene areas about 3 nm in length could be observed in HRTEM micrographs and the results are supported by Raman measurements. The generated defects are mainly point defects of few atoms, which are statistically distributed over the graphene lattice, next to few holes with diameters of 1–3 nm. According to the results of Raman investigations conducted on oxo-G with a degree of functionalization of about 50 %, we propose a defunctionalization pathway based on mobile functional oxo groups that may form CO or CO_2 at existing defects, increasing the size of lattice defects. For conventional GO this process is expected to proceed similarly in hexagonal lattice regions; however, due to the high concentration of lattice defects, already induced during preparation, the growth of an intact graphene lattice is not possible. In contrast, based on the results presented here, oxo-G can even act as a precursor to graphene, which does not require a reducing agent to form a reasonable hexagonal lattice of graphene. The presented materials may act as precursors for membranes used for gas sieving, energy storage, or sensing applications, for which a controlled amount of lattice defects, next to an intact graphene lattice is beneficial. Moreover, thermal processing avoids the introduction of impurities from the reducing agents.

Acknowledgements

S.E. gratefully acknowledges funding from the Deutsche Forschungsgemeinschaft (DFG) via grant EI 938/3-1. We thank SFB 953 funded by the DFG for support.

Conflict of interest

The authors declare no conflict of interest.

Keywords: graphene · oxo-functionalized graphene · Raman spectroscopy · reduction · transmission electron microscopy

How to cite: *Angew. Chem. Int. Ed.* **2017**, *56*, 9222–9225
Angew. Chem. **2017**, *129*, 9350–9353

[1] K. S. Novoselov, A. K. Geim, S. V. Morozov, D. Jiang, Y. Zhang, S. V. Bubonos, I. V. Grigorieva, A. A. Firsov, *Science* **2004**, *306*, 666.
[2] a) A. K. Geim, K. S. Novoselov, *Nat. Mater.* **2007**, *6*, 183; b) D. C. Elias, R. R. Nair, T. M. Mohiuddin, S. V. Morozov, P. Blake, M. P. Halsall, A. C. Ferrari, D. W. Boukhvalov, M. I. Katsnelson, A. K. Geim, K. S. Novoselov, *Science* **2009**, *323*, 610; c) M. J. Allen, V. C. Tung, R. B. Kaner, *Chem. Rev.* **2010**, *110*, 132; d) L. Vicarelli, S. J. Heerema, C. Dekker, H. W. Zandbergen, *ACS Nano* **2015**, *9*, 3428.
[3] Y. Shao, M. F. El-Kady, L. J. Wang, Q. Zhang, Y. Li, H. Wang, M. F. Mousavi, R. B. Kaner, *Chem. Soc. Rev.* **2015**, *44*, 3639.
[4] a) S. K. Balasingam, Y. Jun, *Isr. J. Chem.* **2015**, *55*, 955; b) X. Liu, Z. Li, W. Zhao, C. Zhao, Y. Wang, Z. Lin, *J. Mater. Chem. A* **2015**, *3*, 19148.
[5] a) S. Wu, Q. He, C. Tan, Y. Wang, H. Zhang, *Small* **2013**, *9*, 1160; b) S. S. Varghese, S. Lonkar, K. K. Singh, S. Swaminathan, A. Abdala, *Sens. Actuators B* **2015**, *218*, 160.
[6] a) Z. Wang, S. Eigler, Y. Ishii, Y. Hu, C. Papp, O. Lytken, H.-P. Steinrück, M. Halik, *J. Mater. Chem. C* **2015**, *3*, 8595; b) Y. Yang, C. Han, B. Jiang, J. Iocozzia, C. He, D. Shi, T. Jiang, Z. Lin, *Mater. Sci. Eng. R* **2016**, *102*, 1; c) S. Wu, R. Xu, M. Lu, R. Ge, J. Iocozzia, C. Han, B. Jiang, Z. Lin, *Adv. Energy Mater.* **2015**, *5*, 1500400; d) J. Zhu, D. Yang, Z. Yin, Q. Yan, H. Zhang, *Small* **2014**, *10*, 3480.
[7] a) F. Schedin, A. K. Geim, S. V. Morozov, E. W. Hill, P. Blake, M. I. Katsnelson, K. S. Novoselov, *Nat. Mater.* **2007**, *6*, 652; b) H. Pieper, S. Chercheja, S. Eigler, C. E. Halbig, M. R. Filipovic, A. Mokhir, *Angew. Chem. Int. Ed.* **2016**, *55*, 405; *Angew. Chem.* **2016**, *128*, 413; c) Y. Wang, Z. Li, J. Wang, J. Li, Y. Lin, *Trends Biotechnol.* **2011**, *29*, 205; d) C. Chung, Y. K. Kim, D. Shin, S. R. Ryoo, B. H. Hong, D. H. Min, *Acc. Chem. Res.* **2013**, *46*, 2211.
[8] a) Y. Yang, W. Zhan, R. Peng, C. He, X. Pang, D. Shi, T. Jiang, Z. Lin, *Adv. Mater.* **2015**, *27*, 6376; b) X. Liu, J. Yang, W. Zhao, Y. Wang, Z. Li, Z. Lin, *Small* **2016**, *12*, 4077.
[9] a) H. P. Boehm, A. Clauss, U. Hoffmann, *J. Chim. Phys. Phys.-Chim. Biol.* **1960**, *58*, 110; b) S. Garaj, W. Hubbard, A. Reina, J. Kong, D. Branton, J. A. Golovchenko, *Nature* **2010**, *467*, 190.
[10] a) S. Eigler, M. Enzelberger-Heim, S. Grimm, P. Hofmann, W. Kroener, A. Geworski, C. Dotzer, M. Rockert, J. Xiao, C. Papp, O. Lytken, H. P. Steinrück, P. Müller, A. Hirsch, *Adv. Mater.* **2013**, *25*, 3583; b) P. Vecera, J. Holzwarth, K. F. Edelthalhammer, U. Mundloch, H. Peterlik, F. Hauke, A. Hirsch, *Nat. Commun.* **2016**, *7*, 12411.
[11] a) S. Eigler, *Chemistry* **2016**, *22*, 7012; b) S. Eigler, A. Hirsch, *Angew. Chem. Int. Ed.* **2014**, *53*, 7720; *Angew. Chem.* **2014**, *126*, 7852.
[12] S. Grimm, M. Schweiger, S. Eigler, J. Zaumseil, *J. Phys. Chem. C* **2016**, *120*, 3036.
[13] a) S. Eigler, S. Grimm, M. Enzelberger-Heim, P. Müller, A. Hirsch, *Chem. Commun.* **2013**, *49*, 7391; b) S. Eigler, *Phys. Chem. Chem. Phys.* **2014**, *16*, 19832; c) C. K. Chua, M. Pumera, *Chem. Soc. Rev.* **2014**, *43*, 291.
[14] R. Flyunt, W. Knolle, A. Kahnt, C. E. Halbig, A. Lotnyk, T. Haupl, A. Prager, S. Eigler, B. Abel, *Nanoscale* **2016**, *8*, 7572.
[15] a) S. Eigler, S. Grimm, F. Hof, A. Hirsch, *J. Mater. Chem. A* **2013**, *1*, 11559; b) S. Eigler, C. Dotzer, A. Hirsch, *Carbon* **2012**, *50*, 3666.
[16] S. H. Dave, C. Gong, A. W. Robertson, J. H. Warner, J. C. Grossman, *ACS Nano* **2016**, *10*, 7515.
[17] P. Vecera, S. Eigler, M. Koleśnik-Gray, V. Krstić, A. Vierck, J. Maultzsch, R. Schäfer, F. Hauke, A. Hirsch, *Sci. Rep.* **2016**, *7*, 45165.
[18] a) S. Eigler, *Chem. Commun.* **2015**, *51*, 3162; b) W. Rüdorff, U. Hofmann, *Z. Anorg. Allg. Chem.* **1938**, *238*, 1.
[19] B. Butz, C. Dolle, C. E. Halbig, E. Spiecker, S. Eigler, *Angew. Chem. Int. Ed.* **2016**, *55*, 15771; *Angew. Chem.* **2016**, *128*, 16003.
[20] G. Algara-Siller, O. Lehtinen, A. Turchanin, U. Kaiser, *Appl. Phys. Lett.* **2014**, *104*, 153115.
[21] a) L. G. Cançado, A. Jorio, E. H. M. Ferreira, F. Stavale, C. A. Achete, R. B. Capaz, M. V. O. Moutinho, A. Lombardo, T. S. Kulmala, A. C. Ferrari, *Nano Lett.* **2011**, *11*, 3190; b) M. M. Lucchese, F. Stavale, E. H. M. Ferreira, C. Vilani, M. V. O. Moutinho, R. B. Capaz, C. A. Achete, A. Jorio, *Carbon* **2010**, *48*, 1592.

Manuscript received: April 29, 2017
Accepted manuscript online: May 31, 2017
Version of record online: June 30, 2017

